J. Fluid Mech. (2002), *vol.* 473, *pp.* 201–210.
DOI: 10.1017/S0022112002002501 Printed in the United Kingdom

Sidewall finite-conductivity effects in confined turbulent thermal convection

By ROBERTO VERZICCO

Politecnico di Bari, DIMeG and CEMeC, Via Re David 200, 70125, Bari, Italia

(Received 18 June 2002 and in revised form 28 August 2002)

The effects of a sidewall with finite thermal conductivity on confined turbulent thermal convection has been investigated using direct numerical simulation. The study is motivated by the observation that the heat flowing through the lateral wall is not always negligible in the low-aspect-ratio cells of several recent experiments. The extra heat flux modifies the temperature boundary conditions of the flow and therefore the convective heat transfer. It has been found that, for usual sidewall thicknesses, the heat travelling from the hot to the cold plates directly through the sidewall is negligible owing to the additional heat exchanged at the lateral fluid/wall interface. In contrast, the modified temperature boundary conditions alter the mean flow yielding significant Nusselt number corrections which, in the low Rayleigh number range, can change the exponent of the Nu vs. Ra power law by 10%.

1. Introduction

An aim of research in thermally driven convective turbulence is to try to achieve the largest Rayleigh number (Ra) variation within compact and highly controllable experimental devices. The need for increasing the Rayleigh number as much as possible comes from astrophysical (convection in stars) geophysical (atmospheric and oceanic convection) and industrial (cooling problems) applications with Rayleigh number ranging from 10^6 up to $> 10^{20}$. Another strong motivation is the 'ultimate regime' predicted by Kraichnan (1962) in which the non-dimensional heat transfer Nusselt number Nu increases as $Ra^{1/2}$ (plus logarithmic corrections); this regime should appear at $Ra > 10^{21}$ (Kraichnan, 1962) but has been only indicated (Chavanne *et al.* 1997, among many others), never directly observed for a sufficiently wide range of Rayleigh numbers.

A laboratory realization of a thermally driven turbulent flow consists of two horizontal plates whose vertical spacing is h and representative horizontal dimension L. When a constant temperature difference Δ is established between the plates (the lower being warmer than the upper) fluid motion is generated owing to the buoyancy induced by the fluid thermal expansion. The relevant governing parameters are the Rayleigh number $Ra = g\alpha_f \Delta h^3/(\nu_f k_f)$, the Prandtl number $Pr = \nu_f/k_f$ and the cell aspect ratio $\Gamma = L/h$, where α_f, ν_f and k_f are respectively the isobaric thermal expansion coefficient, the kinematic viscosity and the thermal diffusivity of the working fluid. Given the Ra definition, once the working fluid has been selected (thus fixing ν_f, k_f and α_f) only Δ and h can be varied†; the latter determines the size of the

† ν_f, k_f and α_f could be varied by changing the mean flow temperature, but the different temperature dependence of ν_f and k_f does not generally preserve the Prandtl number and, in addition, does not enable big variations of the Rayleigh number.

experimental apparatus and therefore the cost and the controllability of the set-up; Δ, on the other hand, can be freely varied provided $\alpha_f \Delta$ is small enough (< 0.1–0.2) for the Boussinesq approximation to remain valid (see Niemela & Sreenivasan 2002). Within this scenario, for a given fluid and experimental set-up, Ra can only span one or two orders of magnitude, which is not enough for the above-mentioned problems. A possible alternative is an experimental set-up in which the relative plate distance h can be changed; this, however also modifies the aspect ratio Γ which has been shown to have an influence on the flow dynamics (Wu & Libchaber 1992).

A clever solution to these problems was described in Threlfall (1975) who suggested using helium gas close to the critical-point temperature and modifying its mean pressure. Although very close to the critical point of helium large Prandtl number changes can occur, this allows the variation of ν_f and k_f by several orders of magnitude with limited changes to their ratio (i.e. the Prandtl number) and thus the Rayleigh number is varied by ten or more orders of magnitude with the same apparatus keeping Pr (approximately) constant and retaining the validity of the Boussinesq approximation. In the last two decades this technique has been used by several research teams who have built small-aspect-ratio cylindrical cells of various sizes ($1\,\mathrm{cm} \leqslant h \leqslant 1\,\mathrm{m}$) reaching Rayleigh numbers up to 10^{17} (Niemela *et al.* 2000). The main drawback is that the absolute pressure in these cells must be varied in the range $p_{min} \simeq 70\,\mathrm{Pa}$ to $p_{max} \simeq 1.3 \times 10^6\,\mathrm{Pa}$ and therefore the sidewall must provide, in addition to the thermal insulation, enough mechanical resistance to prevent the cell from deforming or even exploding (or imploding) under the action of the pressure inside. Accordingly these cells have a thin stainless steel sidewall that, even though much less thermally conducting than the copper of the horizontal plates is much more conducting than the inner fluid. In addition, in small-aspect-ratio geometries the sidewall surface is comparable or bigger than the plate surface and therefore its thermal effect not always negligible.

Until very recently the heat flowing through the sidewall was either neglected or accounted for by subtracting the corresponding heat transferred to an empty cell. However, Ahlers (2001) and Roche *et al.* (2001) have shown by phenomenological models that the sidewall correction is not a second order effect and the empty cell correction is not accurate. This was confirmed by Niemela & Sreenivasan (2002) who simulated an idealized two-dimensional convection problem with a conducting side surface and a fly-wheel-like structure in the bulk in order to mimic the mean flow sweeping the walls. These non-negligible effects are not surprising since the thin thermal boundary layers at the horizontal plates make the temperature gradients steeper inside the lateral wall thus increasing its heat flow. On the other hand the modified lateral wall temperature distribution alters the inner flow and therefore the convective heat transfer. This two-way coupling between fluid motion and wall conductivity has never been investigated even though it might be the main reason for the disagreement between different experiments performed in similar conditions.

The main aim of this paper is to evaluate by direct numerical simulations the differences between an ideal set-up with perfectly adiabatic sidewalls and an experiment whose sidewall has finite heat conductivity. It is motivated by some differences observed in the experiments by Chavanne *et al.* (2001); Niemela *et al.* (2000) and Roche *et al.* (2001); therefore, the simulations are performed for a cylindrical cell of aspect ratio $\Gamma = 1/2$; this work, however, is relevant to all thermally driven flows in small-aspect-ratio cells and the results might be used as a guideline for more accurate sidewall corrections.

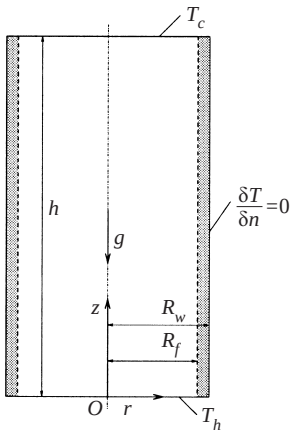

FIGURE 1. Sketch of the cell (vertical plane cut).

2. Problem and set-up

Consider a fluid with physical properties denoted by subscript f contained in a cylindrical cell of inner radius R_f and height h (see figure 1) heated from below by a horizontal plate at constant temperature T_h and cooled from above by a similar plate at temperature T_c with $T_c < T_h$. The wetted surfaces are all no-slip. The lateral wall has a thickness $e = R_w - R_f$ and thermal properties different from those of the fluid and denoted by subscript lw. The flow investigated in this paper is that developing in the cylindrical cell of aspect ratio $\Gamma = 2R_f/h = 1/2$ with a conductive sidewall. Following Roche *et al.* (2001) a wall number $W = 4\lambda_{lw}e/(\lambda_f 2R_f)$ can be defined to quantify the sidewall effects, which represents the ratio of the diffusive thermal resistances of helium and lateral wall layers.

The purpose of the set-up sketched in figure 1 is to mimic the flow conditions of an experiment in which the copper horizontal plates in contact with gaseous helium can be approximated well by constant-temperature surfaces, at least within the range of Rayleigh numbers investigated here. The sidewall is not adiabatic for $r = R_f$ since the conductivity of the steel is much greater than that of the gaseous helium. The lateral wall however can be considered adiabatic at $r = R_w$ owing to the external vacuum jacket preventing any heat exchange but radiation, which at very low temperatures ($\sim 4\,\mathrm{K}$) can be safely neglected.

If V_f is the fluid domain $0 \leqslant z \leqslant h, 0 \leqslant r \leqslant R_f$ and $0 \leqslant \phi < 2\pi$ with ϕ the azimuthal coordinate, and V the total domain the non-dimensional Navier–Stokes equations with the Boussinesq approximation equations are

$$\frac{\mathrm{D}\boldsymbol{u}}{\mathrm{D}t} = -\nabla p + \theta\hat{\boldsymbol{z}} + \left(\frac{Pr}{Ra}\right)^{1/2}\nabla^2\boldsymbol{u}, \quad \nabla\cdot\boldsymbol{u} = 0 \quad \text{on} \quad V_f,$$

$$\frac{\mathrm{D}\theta}{\mathrm{D}t} = \frac{1}{(PrRa)^{1/2}}\frac{\rho_f C_{pf}}{\rho C}\nabla\cdot\left(\frac{\lambda}{\lambda_f}\nabla\theta\right) \quad \text{on} \quad V,$$

where ρ_f, C_{pf} and λ_f with $k_f = \lambda_f/(\rho_f C_{pf})$ are, respectively, the density, constant pressure specific heat and thermal conductivity of the fluid and ρ, C and λ the same quantities for the fluid or the solid (ρ_{lw} C_{lw} and λ_{lw}) depending on the point in the domain. The following material properties have been assumed, respectively for gaseous helium and stainless steel at $T = 4.5\,\mathrm{K}$: $\lambda_f = 0.0087\,\mathrm{W\,K^{-1}\,m^{-1}}$, $(\rho C_p)_f = 3190\,\mathrm{J\,K^{-1}\,m^{-3}}$, $\lambda_{lw} = 0.4\,\mathrm{W\,K^{-1}\,m^{-1}}$ and $(\rho C)_{lw} = 30000\,\mathrm{J\,K^{-1}\,m^{-3}}$ (J. Niemela and

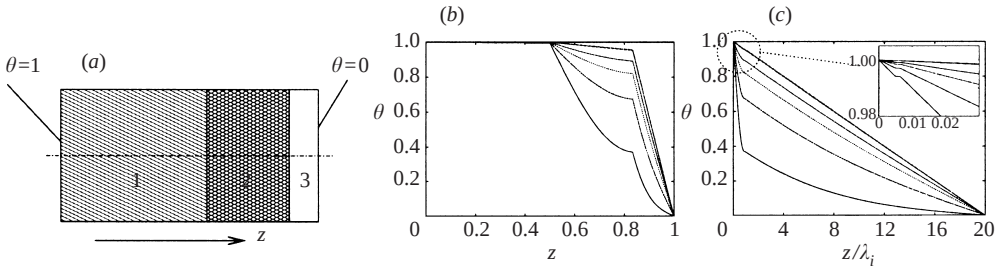

FIGURE 2. Solution of the conductive heat transfer problem in discontinuous media. Medium 1 is copper, 2 stainless steel and 3 gaseous helium. The solutions in (b, c) in are reported at $t = 2.5$, 5, 7.5, 10, 20 and 40, respectively from the lower line to the upper one.

P. Roche, Personal Communication).† $\hat{\boldsymbol{z}}$ is the unit vector pointing in the opposite direction to gravity, $\boldsymbol{u}$ the velocity vector, p the pressure (separated from its hydrostatic contribution) and θ the non-dimensional temperature. The equations have been made non-dimensional using the free-fall velocity $U = \sqrt{g\alpha_f \Delta h}$, the distance between hot and cold plates h and their temperature difference $\Delta = T_h - T_c$; the non-dimensional temperature θ is defined as $\theta = (T - T_c)/\Delta$ so that $0 \leqslant \theta \leqslant 1$.

The above equations have been written in a cylindrical coordinate frame and discretized on a staggered mesh by central second-order-accurate finite-difference approximations. The numerical method is described in Verzicco & Camussi (1999) where further details of the numerical procedure can be found, the only relevant change being the presence of an immersed boundary procedure (Fadlun *et al.* 2000) allowing the solution of the momentum and temperature equations on different domains.

As the physical problem and the structure of the numerical code are essentially the same as that of Verzicco & Camussi (1999, 2003) we have used those simulations to assess the resolution requirements and to validate the numerical procedure. In particular grids from $33 \times 49 \times 97$ up to $97 \times 65 \times 257$ nodes, respectively in the azimuthal, radial and vertical directions, with a non-uniform mesh in r and z, have been used for Ra in the range 2×10^6–2×10^9; this yielded a mesh size between 1 and 2 Kolmogorov scales in the bulk of the flow and 6–10 nodes in the thermal boundary layer which was always thinner than the viscous layer (Verzicco & Camussi 2003). For the simulations with a conducting sidewall 5 nodes were placed in the wall thickness. As a grid refinement check one case at $Ra = 2 \times 10^8$ has been run with the grids $97 \times 65 \times 193$ and $49 \times 49 \times 129$ obtaining a Nusselt number, respectively, of 48.18 ± 2.87 and 48.40 ± 2.98. Finally, since there is the new feature of the temperature equation for a variable-property medium an additional validation test has been performed; although the validation is not directly related to the main problem it provides an analytical benchmark for the simulation of the heat conduction in materials with non-constant properties. By turning off the momentum equation and setting the material properties so that three cylinders of different material are arranged concentrically (figure 2*a*), starting from $\theta = 0$ everywhere and with the given boundary conditions, the temperature must attain a steady state with a linear piecewise profile (figure 2*b*). In addition, when the spatial coordinate is scaled by

† For the oxygen-free copper of the horizontal plates the material parameters are $\lambda_{cu} = 1000\,\mathrm{W\,K^{-1}\,m^{-1}}$ and $(\rho C)_{cu} = 890\,\mathrm{J\,K^{-1}\,m^{-3}}$ yielding a thermal diffusivity k_{cu} which is, respectively, 10^5 and 10^6 times bigger than that of the fluid and the sidewall. This explains why, for this range of Rayleigh numbers, the temperature on the horizontal plates can be safely considered constant.

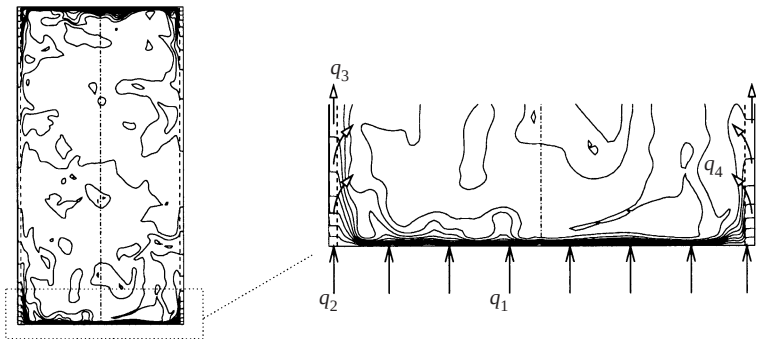

FIGURE 3. Instantaneous vertical snapshot of the temperature distribution ($\Delta\theta = 0.05$) at $Ra = 2 \times 10^8$, $Pr = 0.7$ and $W = 3.678$. q_1 indicates the heat flowing from the plate to the fluid, q_2 from the plate to the sidewall, q_3 only through the sidewall and q_4 from the sidewall to the fluid (q_i are the heat flux densities).

the local thermal conductivity the three segments must collapse onto a unique line (figure 2*c*); these results, for the case of copper, steel and helium, confirm the analytical prediction for the pure conductive problem.

The length of each run was fixed by the statistics convergence; in particular, requiring error bars of the order of 3% on the heat transfers from the horizontal plates (see § 3 for the various definitions) the simulation of 100–170 large-eddy-turnover times T_l (with $T_l = 2h/U$) was needed for $2 \times 10^6 \leqslant Ra \leqslant 2 \times 10^9$. Verzicco & Camussi (2003) showed that these simulation lengths are also sufficient for the accurate evaluation of the second-order statistics.

3. Results

The global heat transport in the flow, normalized by the pure conductive contribution, is expressed by the Nusselt number that can be written as $Nu = 1 + \sqrt{RaPr}\langle u_z\theta\rangle$; the angular brackets indicate an average over time and over the whole fluid domain V_f. If the sidewall were perfectly adiabatic, this definition would be, on average, equivalent to the normalized heat flux density evaluated at the wetted hot and cold plates $Q_f = \widetilde{\partial\theta/\partial z}|_w$ where $|_w$ indicates that the derivative is computed at the wall and the tilde implies an average in time and over the fluid/plate surface ($0 \leqslant r \leqslant R_f$). In the present case, in contrast, part of the heat can flow through the side solid wall and the two Nusselt definitions do not match. The quantity $Q = \overline{(\lambda/\lambda_f)\partial\theta/\partial z}|_w$, with the overbar indicating an average in time and over the whole plate surface ($0 \leqslant r \leqslant R_w$) and λ equal to λ_f or λ_{lw} depending on the surface element, is the total heat flux density input of the system. We can now separate the heat flux entering the fluid directly from the horizontal plate Q_f from that escaping through the sidewall $Q_w = Q - Q_f$ (see figure 3); only part of Q_w flows from the hot to the cold plate directly through the sidewall since the rest enters the fluid through the lateral wetted surface (figure 3); this additional heat flux in turn changes the motion inside the cell thus establishing a feedback between heat transfer and flow configuration.

In a laboratory experiment Q is the only measurable quantity and Q_w must be estimated. Ahlers (2001) and Roche *et al.* (2001) propose simplified models to quantify Q_w although former correctly points out that the assumption of Q_w as the relevant correction deserves further investigation. We will show that the difference between Nu

Ra	Q	Nu	Nu_{id}	f	C
2×10^6	14.98	13.42	10.79	0.144	0.243
2×10^7	27.22	24.80	20.66	0.138	0.200
2×10^8	49.28	48.18	41.32	0.116	0.166
2×10^9	107.44	104.53	94.14	0.091	0.110

TABLE 1. Heat transfer and related quantities for the flow at $Pr = 0.7$ and $W = 0.919$.

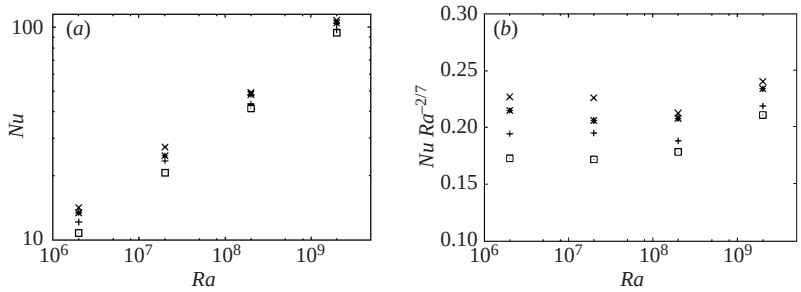

FIGURE 4. (a) Heat transfer vs. Ra, (b) compensated heat transfer at $Pr = 0.7$ and $W = 0.919$: □, Nu_{id}; +, $(1-f)Q$; *, Nu; ×, Q.

and Q is smaller than Q_w since part of the heat initially flowing through the sidewall enters the flow through the lateral surface.

The situation is considerably more complex when the ideal adiabatic sidewall and the real flow cases are compared. In fact, the modified temperature conditions on the sidewall produce a different mean flow and therefore a different convective heat transport. In this context, the only way to quantify the sidewall effect is by a comparison of the finite conductivity results with 'ideal flow' simulations in which the wall has zero thickness ($R_w = R_f$) and therefore the adiabatic boundary condition is applied at the wetted side surface ($r = R_f$). For the latter flows the *ideal* Nusselt $Nu_{id} = 1 + \sqrt{RaPr}\langle u_z \theta \rangle$ can be computed and the quantity $C = (Nu - Nu_{id})/Nu_{id}$ is taken as the net sidewall effect. In table 1 we report the values of these quantities including a factor $f = (Q - Q_f)/Q = Q_w/Q$ which Ahlers (2001) uses to correct the sidewall effect $\mathcal{N} = (1-f)Q$; every simulation is for a wall number $W = 0.919$ obtained from a cell with $e = 0.0025h$ and $\lambda_{lw}/\lambda_f = 46$ (stainless steel and gaseous helium).

In figure 4 we report the variation of the different heat transfer definitions with Ra showing that, depending on the particular quantity, the slopes can be substantially altered; with an error bar of the order of $\pm 4\%$ all data approximately agree and the differences might be interpreted as 'scatter'. However, the present quantities have been computed with a total error bar of the order of 3–4%: this implies that the Q vs. Ra relation can be fitted with a 0.288 exponent power law, while the exponent is 0.309 for the Nu_{id} vs. Ra data. The differences are even more pronounced for the local slopes and this is particularly critical for this flow since, as observed by Verzicco & Camussi (2003), there is evidence of a transition near $Ra \approx 10^9$, due to a change of the mean flow structure. This is detected in the compensated Nusselt number as a continuous increase of the slope with respect to the 2/7 value; therefore, when in addition to error bars further scatter is introduced by the sidewall this transition might be hidden or in the wrong position. Further comments on the data of table 1 are that the differences 0 between Q and Nu are much smaller than the correction given by f, thus confirming

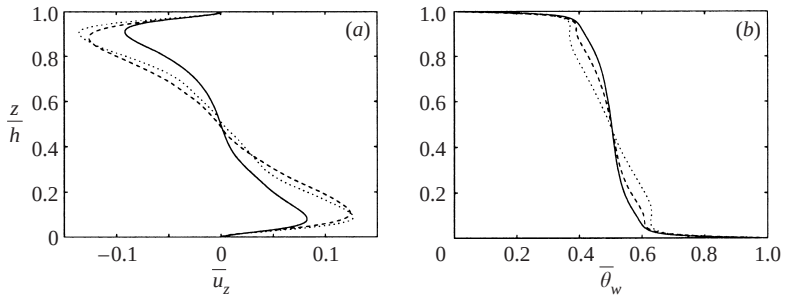

FIGURE 5. Vertical profiles of (*a*) mean vertical velocity at $r/h = 0.235$ and (*b*) wall temperature $r/h = 0.25$ at $Ra = 2 \times 10^8$ and $Pr = 0.7$; ———, $W = 0$; – – – –, $W = 0.919$; ·····, $W = 3.678$.

that a large part of the heat current Q_w flows into the fluid through the sidewall interface. The factor f decreases with Ra less than the prediction by Ahlers (2001) and an extrapolation to higher Ra would give a correction of the order of 5% at $Ra \approx 10^{11}$; on account of the previous arguments, however, the difference between Q and Nu would be negligible since it is already only 2.5% at $Ra = 2 \times 10^9$. The results obtained by Niemela & Sreenivasan (2002) are in agreement with those by Ahlers (2001) and this is consistent with the fact that also in their paper the mean flow, and therefore the sidewall boundary layer, was imposed from experimental measurements.

The heat transport differences are much more pronounced when Nu is compared with the ideal value Nu_{id}; in this case, C ranges from 24% to 11% for $2 \times 10^6 \leqslant Ra \leqslant 2 \times 10^9$ and an extrapolation yields $C \approx 5\%$ at $Ra \approx 10^{11}$. As previously mentioned these differences are due to changes in the mean flow which will be analysed in detail. According to figure 3 several effects can be ascribed to the conductive lateral surface; in particular, the heat flowing through the sidewall causes the horizontal thermal boundary layers to thicken in the external radial region, thus locally decreasing the heat exchange. On the other hand, the lateral thermal layer acts as an additional forcing on the mean flow structures which are modified compared to the ideal adiabatic sidewall flow. Verzicco & Camussi (2003) have observed that for $Ra \leqslant 10^{10}$ in this geometry the mean flow consists of an asymmetric large-scale roll completely filling the cell superposed on axisymmetric toroidal rings attached to the horizontal plates. If the sidewall is heated (or cooled) the vertical thermal layers add buoyancy to the rings and strengthen their circulation. These strengthened rings, in turn, drive the fluid from the plates to the lateral wall thus further heating or cooling this surface; evidence of these phenomena is given in figures 5 and 6 where the results are shown for two different values of W and compared with the ideal flow. Note that the value $W = 3.678$ was obtained assuming stainless steel in contact with gaseous helium and $e = 0.01h$ which for a height $h = 10\,\text{cm}$ implies a sidewall thickness $e = 1\,\text{mm}$: at $Ra = 2 \times 10^8$ the difference between Q and Nu was 4.6% while the corrections $C = 0.245$ and $f = 0.223$ were twice value for the thinner wall case ($W = 0.919$). The sensitivity of the corrections to the wall thickness could be the reason for the scatter of experimental results obtained in (apparently) similar conditions.

Table 1 shows that the effect of the lateral wall on the heat transfer decreases as Ra increases and this is due to the increase of the effective thermal conductivity of the fluid $\lambda_{eff} = Nu\lambda$ which eventually becomes larger than that of the wall. Nevertheless, the consequences of the modified temperature boundary conditions on the mean flow persist at high Rayleigh numbers also and this is why at $Ra = 2 \times 10^9$ the correction C is more than 11% even though the difference between Q and Nu is only 2%. In figure 7

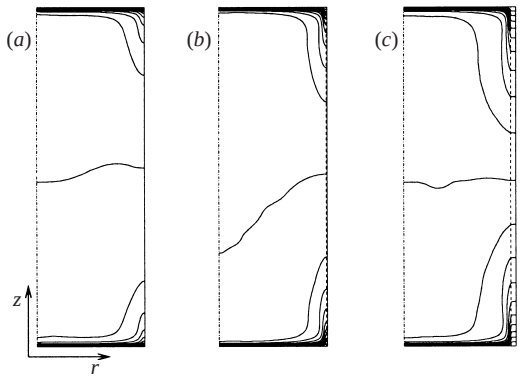

FIGURE 6. Mean temperature fields at $Ra = 2 \times 10^8$, $Pr = 0.7$; (*a*) $W = 0$, (*b*) $W = 0.919$ and (*c*) $W = 3.678$. $\Delta\theta = 0.05$.

we report the comparison between ideal and finite-conductivity flows for velocity and dissipation fields at $Ra = 2 \times 10^8$. The flow topology is the same in both cases but the velocity peaks are very different (50% for the radial velocity at the plates and 30% for the vertical velocity). An important observation is that in the junction regions (see figure 7) the fluid also exchanges heat with the sidewall and, owing to buoyancy, it gains additional momentum compared to an insulating wall; this is a cause of mean flow modification that, in turn, affects the Nusselt number. Another consequence is the alteration of the sidewall boundary layers and therefore of the kinetic energy and temperature variance dissipation rates. This might be relevant to the recent theory by Grossmann & Lohse (2000) that separates different flow regimes depending on the dominant dissipation contributions (bulk or boundary layer). Accordingly, since flows in low-aspect-ratio cells have a substantial dissipation input from the sidewall, this theory might possibly need corrections accounting for the finite conductivity.

It is interesting to note, both from figures 6 and 7(*d*), that the overall effect of a conducting sidewall is a 'continuation' of the plates on part of the vertical surface with an increase of the active heat exchange surface. This was conjectured by Roche *et al.* (2001) who indicated this effect as the relevant correction to be accounted for; in particular, using experimental data with different wall numbers W they were able to compute a 'corrected' Nusselt Nu_c from the implicit relation $Nu_c = Q/\{1+A^2/(\Gamma Nu_c)[\sqrt{1+(2W\Gamma Nu_c/A^2}]-1\}$, with A depending on the aspect ratio of the cell and on the working fluid. They used $A = 0.80$ yielding, with the present data, differences between Nu_c and Q in the range 37.4–14.6% for $2 \times 10^6 \leqslant Ra \leqslant 2 \times 10^9$. If Nu_c is interpreted as Nu_{id} we see that the correction is in very good agreement with the values of table 1. Indeed, Roche *et al.* (2001) for a cell with $e = 0.0025h$ and a stainless steel/gaseous helium interface computed $W = 0.6$ which in their formula gives corrections 28.4–11.3% for $2 \times 10^6 \leqslant Ra \leqslant 2 \times 10^9$. These values underestimate the correction, thus indicating that their fit procedure with different values for W might give a slightly different estimate for A.

One additional simulation was carried out at $Ra = 2 \times 10^8$, $Pr = 4$ and $W = 0.013$ with the aim of checking the effect of the sidewall when the working fluid is water. Since the thermal conductivity of water is about 60 times larger than that of gaseous helium, it is reasonable to expect a negligible effect of the steel lateral surface whose thermal conductivity is 0.65 times smaller than that of water (data from Ahlers 2001). This is partially confirmed by the factor $f = 0.015$ which is less than one fifth of the corresponding value for helium; nevertheless, the difference between Nu and Nu_{id}

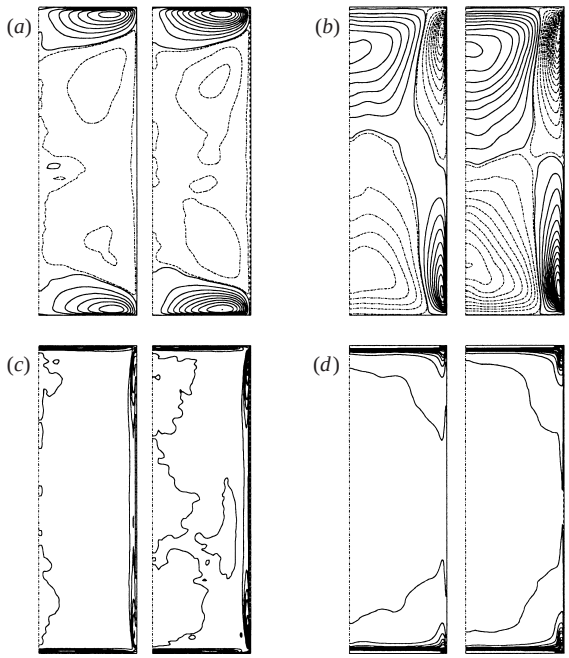

FIGURE 7. Mean fields at $Ra = 2\times10^8$ and $Pr = 0.7$; (*a*) u_r, (*b*) u_z, (*c*) local kinetic energy dissipation rate ϵ, (*d*) local temperature variance dissipation rate N. $\Delta u = \pm0.01$. For the dissipations there are 10 contour levels between the maximum value and 20% of the maximum and 5 lines in the remaining range. Left: ideal adiabatic sidewall, right: sidewall with $W = 0.919$.

is still appreciable ($C = 0.103$) owing to the 'extension' of the plate surface over the junction region. While this finding deserves further investigation, especially for the dependence on Ra, it confirms that the consequences of the modified temperature boundary conditions are much more severe on the heat transfer than the flux through the sidewall.

4. Conclusions

In this paper we have investigated the effect of finite sidewall conductivity in turbulent thermal convection. Using direct numerical simulation we have separated the heat flux from the lower heated plate into a part entering the fluid Q_f and another contribution through the lateral wall Q_w. According to Ahlers (2001), Q_w is larger than the estimate given by the pure conductive assumption since the thermal boundary layer at the horizontal plates increases the local thermal gradient at the plate/sidewall junction. Nevertheless the factor $f = Q_w/Q$ does not give a correct estimate of the spurious heat flux since an additional thermal boundary layer forms at the vertical surface that exchanges further heat with the fluid. As a consequence the heat flowing only through the sidewall without entering the fluid is much less than Q_w and at $Ra = 2\times10^9$, $Pr = 0.7$ and $W = 0.919$ it is only of the order of 2% of Q. A major effect of the spurious heat flux is the generation of a lateral vertical thermal boundary layer that, adding buoyancy (and momentum) to the fluid, strengthens the mean flow and changes the heat transfer. These phenomena are accounted for by the factor C which gives the relative difference between the heat transfer in a flow with an ideal adiabatic sidewall and a flow with a conductive lateral wall.

As observed by Roche *et al.* (2001) its macroscopic effect is an 'extension' of the plate surface and an enhancement of the heat transfer. The consequence for the Nu vs. Ra relation is a decrease of the power law exponent with respect to the ideal flow; nevertheless the difference between Nu_{id} and Nu (or Q) decreases with Ra and it becomes negligible ($O(5\%)$) for $Ra = O(10^{11})$. Niemela & Sreenivasan (2002) compute a correction that should be intermediate between f and C since they account for the heat flowing from the sidewall to the fluid but they do not consider the mean flow change (which is allowed to scale with Ra without change in form); the qualitative behaviour of that correction is consistent with the present and previous findings.

As a final comment we conclude that the relevant effect of the sidewall conductivity is the modification of the mean flow through the changed temperature boundary conditions and this is responsible for the difference between Nu_{id} and Q, the latter being the quantity available from experimental measurements. This difference is the correction to the 'raw' Q since the experiments are aimed at approximating as closely as possible an adiabatic sidewall. On the other hand to measure how much of the input heat goes in the flow through the bottom plate, regardless of the sidewall nature, then the factor f must be used.

An additional consequence of this phenomenon is a modification of the dissipation distributions which might have implications for the recent theory by Grossmann & Lohse (2000).

The author is indebted to R. Camussi, J. Niemela, P. Roche and G. Ahlers for fruitful discussions. The paper was prepared with the financial support of CEMeC of Politecnico di Bari. The technical support of CASPUR (Consorzio interuniversitario per le Applicazioni di Supercalcolo Per Università e Ricerca) provided by Drs F. Massaioli and G. Amati is gratefully acknowledged.

REFERENCES

Ahlers, G. 2001 Effect of sidewall conductance on heat-transport measurements for turbulent Rayleigh–Benard convection. *Phys. Rev.* E **6302**(2), 5303 U7–U9.

Chavanne, X., Chillà, F., Castaing, B., Hebral, B., Chabaud, B. & Chaussy, J. 1997 Observation of the ultimate regime in Rayleigh–Bénard convection. *Phys. Rev. Lett.* **79**, 3648–3651.

Chavanne, X., Chillà, F., Chabaud, B., Castaing, B. & Hebral, B. 2001 Turbulent Rayleigh–Bénard convection in gaseous and liquid He. *Phys. Fluids* **13**, 1300–1320.

Fadlun, E. A., Verzicco, R., Orlandi, P. & Mohd-Yusof, J. 2000 Combined immersed-boundary/finite-difference methods for three-dimensional complex flow simulations. *J. Comput. Phys.* **161**, 35–60.

Grossmann, S. & Lohse, D. 2000 Scaling in thermal convection: a unifying theory. *J. Fluid Mech.* **407**, 27–56.

Kraichnan, R. H. 1962 Turbulent thermal convection at arbitrary Prandtl number. *Phys. Fluids* **5**, 1374–1389.

Niemela, J. J., Skrbek, L., Sreenivasan, R. R. & Donnelly, R. J. 2000 Turbulent convection at very high Rayleigh numbers. *Nature* **404**, 837–841.

Niemela, J. J. & Sreenivasan, K. R. 2002 Confined turbulent convection. *J. Fluid Mech.* (submitted).

Roche, P. E., Castaing, B., Chabaud, B., Hebral, B. & Sommeria, J. 2001 Sidewall effects in Rayleigh–Benard experiments. *Eur. Phys. J.* B **24**, 405–408.

Threlfall, D. C. 1975 Free convection in low temperature gaseous helium. *J. Fluid Mech.* **67**, 17–28.

Verzicco, R. & Camussi, R. 1999 Prandtl number effects in convective turbulence. *J. Fluid Mech.* **383**, 55–73.

Verzicco, R. & Camussi, R. 2003 Numerical experiments on strongly turbulent thermal convection in a slender cylindrical cell. *J. Fluid Mech.* (to appear).

Wu, X. Z. & Libchaber A. 1992 Scaling relations in thermal turbulence: The aspect-ratio dependence. *Phys. Rev.* A **45**, 842–845.